General Disclaimer

One or more of the Following Statements may affect this Document

- This document has been reproduced from the best copy furnished by the organizational source. It is being released in the interest of making available as much information as possible.

- This document may contain data, which exceeds the sheet parameters. It was furnished in this condition by the organizational source and is the best copy available.

- This document may contain tone-on-tone or color graphs, charts and/or pictures, which have been reproduced in black and white.

- This document is paginated as submitted by the original source.

- Portions of this document are not fully legible due to the historical nature of some of the material. However, it is the best reproduction available from the original submission.

GRUMMAN AEROSPACE CORPORATION

RESEARCH & DEVELOPMENT CENTER

32319

REPORT RE-691

SPAR X TECHNICAL REPORT FOR EXPERIMENT 76-22
DIRECTIONAL SOLIDIFICATION OF MAGNETIC COMPOSITES

NOVEMBER 1984

Post-Flight Technical Report on Contract NAS8-32319 *per DRA*

prepared by

James Bethin

Materials & Structural Mechanics Directorate

Research and Development Center
Grumman Aerospace Corporation
Bethpage, New York   11714

prepared for

George C. Marshall Space Flight Center
National Aeronautics and Space Administration
Marshall Space Flight Center, Alabama   35812

Approved by:
Richard A. Scheuing, V.P.
Director, R&D Center

ABSTRACT

The effects of gravity on Bridgman-Stockbarger directional solidification of off-eutectic Bi/MnBi has been studied in reduced gravity ($10^{-4}g_e$) aboard the SPAR X flight and compared to normal-gravity investigations and previous eutectic Bi/MnBi SPAR flight experiments. The directional solidification of off-eutectic Bi/MnBi results in either a dendritic structure connected with local cooperative growth or, with the proper solidification conditions, a coupled low volume fraction faceted/non faceted aligned rod eutectic whose Mn macrosegregation, MnBi rod size, interrod spacing, thermal and magnetic properties are sensitive functions of the solidification processing conditions.

Two hypoeutectic and two hypereutectic samples were solidified during 605 s of furnace travel, with an initial 265 s low-gravity interval, at a growth rate 11 cm/h. Comparison earth-gravity samples were solidified in the same furnace assembly under identical processing conditions. Macrosegregation in the low-$\bar{g}$ samples determined by magnetic measurements, microstructural analysis, X-ray fluorescence, and chemical spectrophotometric absorbance, was consistent with a metastable increase in Mn solubility in the Bi matrix, in partial agreement with previous Bi/MnBi SPAR findings of MnBi volume reduction. Smaller mean rod diameter and interrod spacing were found in solidification in low gravity, as compared to earth gravity, in agreement with previous SPAR findings. In addition, in normal gravity, Mn macrosegregation results for the hypoeutectic samples suggest that the thermal instability led to greater convection than did the induced solutal instability. Convection in earth gravity is suggested as an explanation of morphological differences between normal- and low-gravity solidification. This explanation is consistent with a possible change in the equilibrium solid solubility limit of Mn in Bi observed in low gravity.

CONTENTS

ILLUSTRATIONS

TABLES

INTRODUCTION

This work compares the Bridgman-Stockbarger directional solidification of the Bi/MnBi off-eutectic system in low gravity to that in earth gravity. Low gravity provides both a scientifically revealing and potentially advantageous modification of controlled directional solidification of binary alloys in earth gravity. In alloys where the melt density depends on temperature and on solute concentration, convection which consequently occurs in the melt in earth gravity is substantially reduced in low gravity. Of particular interest is the role of convection in solute macrosegregation and in the aligned morphology observed in off-eutectic cooperatively grown systems.

Controlled plane-front directional solidification near the Bi/MnBi eutectic (2.7 a/o or 0.72 w/o Mn) produces an aligned (cooperatively grown) array of highly magnetic MnBi rods, which are often faceted and chevron-shaped in cross section and have very large aspect ratios, in a Bi-matrix which appears unfaceted. The morphology (and therefore the magnetic properties) and the thermal history during growth have been shown (Ref. 1-5) to be sensitively dependent on the growth parameters and the degree of convection. For example, in an earth-gravity study of the solidification of the Bi/MnBi off-eutectic system, different orientations of the solidification direction with respect to the gravity vector have resulted in different degrees of thermal and solutal convective flow as reflected in macrosegregation curves. Previous low-gravity experiments (Ref. 3 and 4) conducted on SPAR flights VI and IX have shown reduced interrod spacing and rod diameters in low-gravity processed samples. In addition, a lower volume fraction of the MnBi phase and a larger interfacial undercooling, i.e., a lower solidification temperature, was found for low-gravity compared to earth-gravity samples. It appears unlikely that either a modified temperature gradient (Ref. 6) or a fluctuating interface speed induced by convective flow (Ref. 7 and 8) will account for the reduction in the interrod spacings. The lack of understanding of the convective, thermal, and morphological effects of low-gravity processing have led to this directional solidification experiment in low and one gravity for the Bi/MnBi off-eutectic system.

1

Samples of 0.49 w/o and 0.90 w/o Mn were grown up and down with respect to the gravity vector, providing different degrees of thermal and solutal convection on the ground. The nominal value of the furnace velocity was 11 cm/h and that of the thermal gradient in the liquid ahead of the interface was 140°C/cm. This moderate furnace velocity was chosen to reach a balance between the desire to obtain a cooperative morphology using a low velocity and the need to solidify a useful length of sample in the low-gravity period of 5 min. Also, the highest possible thermal gradient was used to maintain a planar freezing interface and thus maximize the extent of the cooperative region in each sample. The objectives of this investigation included:

(1) Determining the effect of a reduction in gravity on the macrosegregation of Mn, the thermal history during growth (cooling rate and undercooling), and the morphology of cooperatively grown off-eutectic samples.

(2) Determining the extent to which a reduction in gravity may alter the degree to which cooperative growth may be further stabilized.

(3) Determining areas of special interest or problems associated with the Bi/MnBi off-eutectic system or hardware in preparation for longer periods of low-gravity Bi/MnBi processing experiments aboard the space shuttle.

OFF-EUTECTIC SOLIDIFICATION

Gravity-induced Mn macrosegregation throughout the length of a plane-front solidified Bi/MnBi sample has its origin in the thermal and/or solutal convection in the melt during the growth of the solid. When solidification of a sample in the Bridgman-Stockbarger method proceeds with the cold zone below the hot zone, a relative thermal stability is achieved (growth up). An unstable thermal situation is obtained in growth down, when the hot zone is below the cold zone, which induces thermal convective flow. It is also expected that a Bi-rich sample will exhibit solutal convection during solidification in the growth-up configuration in earth gravity. This is expected because a Bi-rich sample rejects Mn from the solidification front as growth proceeds, up to the point where no Mn gradient exists in the liquid (i.e., the bulk liquid composition equals the eutectic composition). Similarly, a Mn-rich sample will reject Bi at the front resulting in a solutally unstable situation for growth down in earth gravity giving rise to solutal convection. These types of convection give rise to macrosegregation in the Bi/MnBi off-eutectic system which has been treated theoretically with a simplified model by Verhoeven and Homer (Ref. 9). The result is an analytical expression describing the average solid composition as a function of the fraction of the sample solidified. For a cooperatively grown, directionally solidified sample, the parameters from the fit to the experimental macrosegregation data give a measure of the degree of convective versus diffusive control over the solute redistribution.

A third source of macrosegregation which must be dealt with in this system is that arising from what is here termed gravity-driven Stokes migration. In 1-$\bar{g}$ growth up of a Mn-rich sample, MnBi dendrites, which will form at the interface if the dendritic to cooperative transition has not been reached (see below), may be sheared off by convective flow or thermal instabilities and float toward the top of the melt, driven by buoyancy. Dendrites may also grow in the melt near the interface in the presence of constitutional supercooling and float toward the top of the melt. These migrated dendrites may re-dissolve or remain and possibly nucleate further dendrites as the interface again approaches. Thus Stokes migration or flow

3

could lead to a gross disturbance of the Mn macrosegregation in these cases. Stokes migration effects have been noted previously, for example, in monotectic solidification (Ref. 10 and 11) and in dendritic growth in the Sn-Pb system (Ref. 12).

A previous study of the solidification of the Bi/MnBi off-eutectic system in earth gravity has shown that under certain solidification conditions samples solidify first with MnBi dendrites (hypereutectic) or with Bi solid solution dendrites (hypoeutectic) and undergo a transition to cooperative growth as the solidification proceeds (Ref. 1). A quantitative description of the position at which dendrites disappear is possible. Some inconsistencies in the experimental results of Table 1 of Ref. 1 have been corrected and a re-evaluation of those results have led us to replace Fig. 7 of Ref. 1 with Fig. 1 here. The solid lines for Bi-rich and Mn-rich cases are based on the assumption of dendritic growth for even negligible constitutional supercooling. The zero constitutional supercooling criterion (Ref. 13) is described by

$$G/V = -m(C_E - C_S)/D \qquad (1)$$

where G is the thermal gradient in the liquid, V is the interface velocity, m is the slope of the appropriate liquidus, C_E is the eutectic composition, C_S is the average solid composition at a particular cross-sectional position, and and D is the diffusivity of Mn in the melt, assumed to be 2×10^{-5} cm^2/s. In the Bi-rich region the disappearance of dendrites is described well by Eq (1). Although scatter is large in the Mn-rich system, it seems clear that the criterion of no constitutional supercooling with the currently used value of D underestimates the cooperative compositional range. This trend has been noted by other workers (Ref. 14) and might be better accounted for by a competitive growth model (Ref. 15 and 16). This theory finds that a finite constitutional undercooling is possible at the interface before plane front growth becomes unstable. The dashed line is a linear least squares fit of the Mn-rich data which has been constrained to go through the eutectic composition and G/V = 0 point. In order to directionally solidify an entire sample without dendrites, G and V must be chosen to place the entire Mn composition profile, including the effects of convective flow on macrosegregation, above the data in Fig. 1.

4

Mn CONCENTRATION (C_{tr}), w/o Mn

○   GROWTH UP

△   GROWTH DOWN

——— CONSTITUTIONAL SUPERCOOLING CRITERION

— — — L.S. FIT TO Mn-RICH DATA CONSTRAINED
TO GO THROUGH G/V = 0 & C_{tr} = 2.7 a/o Mn
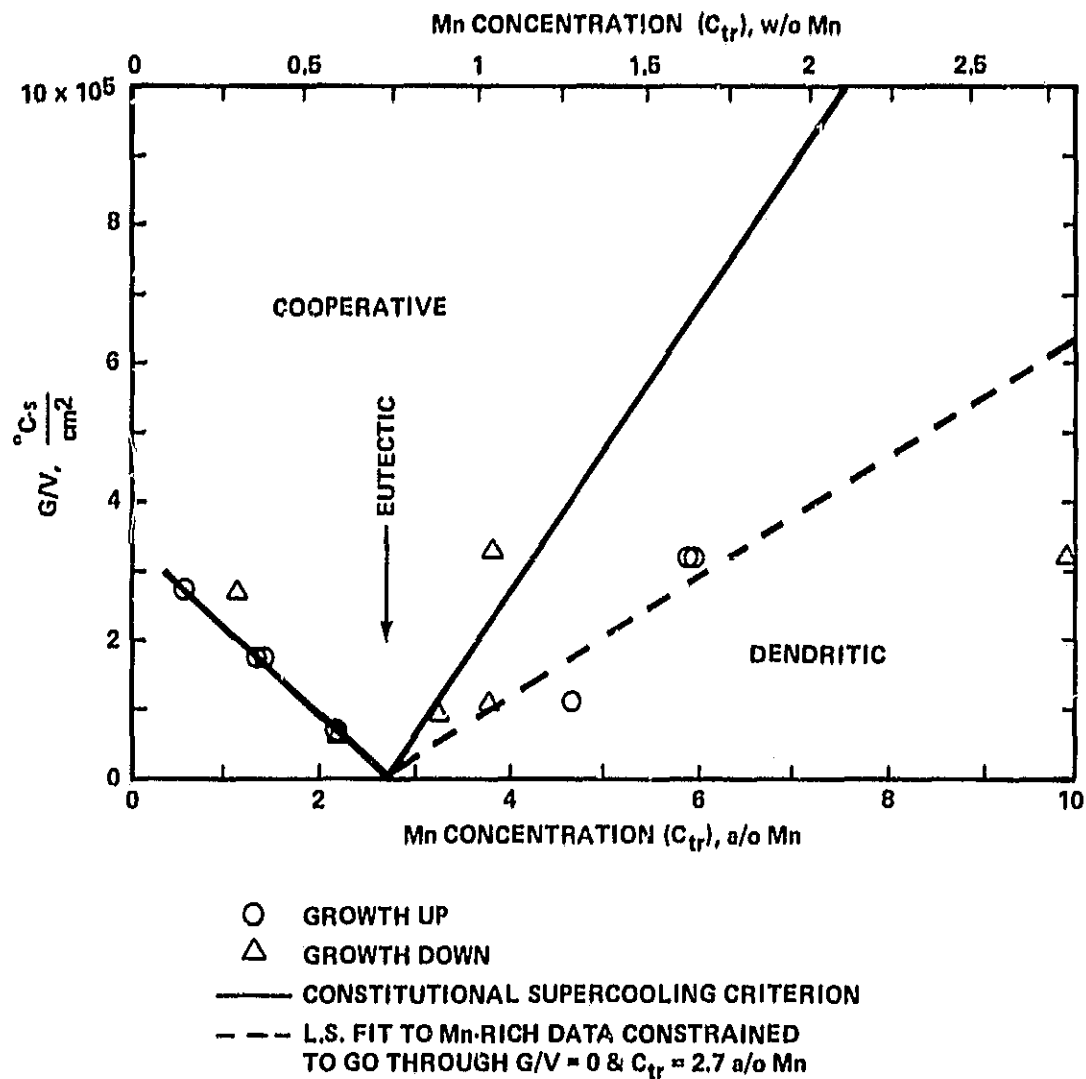
1330-001(T)

Fig. 1 G/V vs Average Mn Composition at the Position
of Dendritic-to-Cooperative Transistion (C_{tr}) in 1-ḡ

EUTECTIC SOLIDIFICATION

Low-gravity solidification of eutectic Bi/MnBi has been studied previously aboard the SPAR VI and SPAR IX flight experiments (Ref. 3 and 4) with very interesting results which have significance for the solidification of the off-eutectic system. These results were contrasted to earth-gravity solidification results and revealed:

o   A decrease in the mean MnBi rod diameter, d, and interrod spacing, λ, by almost 50% aboard SPAR IX and 40% in SPAR VI;

o   Lower volume fraction of MnBi by about 8% in SPAR IX and about 7% in SPAR VI;

o   Bi-rich like macrosegregation in low-gravity solidification of "eutectic" compositions;

o   Increased interfacial undercooling, ΔT, i.e., lower solidification temperature, in low-gravity solidification aboard SPAR IX, by about 50%.

Quenisset and Naslain (Ref. 17) have developed a theoretical approach to lamellar eutectic growth which includes the effect of gravitationally induced convection parallel to the solidification interface. The artificial, simplifying assumption of a stagnant boundary layer is dropped, with the new model leading to a characteristic diffusional length, $\lambda/2$, smaller than found in other growth models. This model predicts a decrease in λ and an increase in ΔT as the fluid flow velocity decreases, such as is expected in low gravity. Baskaran, et al (Ref. 8) found a similar result. This is in qualitative agreement with the previous SPAR experimental eutectic findings.

An effect of an increased undercooling in low gravity would be an adjustment in the phase diagram near the eutectic and the solid solubility limit of Mn in Bi. Metastable extensions of the various phase lines to accommodate the lower freezing temperature could change both the eutectic composition and the solid solubility limit. These compositional changes may be substantial since this eutectic system has a rather low minor phase volume

6

fraction. Therefore, samples with 0.72 w/o Mn (itectic in earth gravity)
might conceivably directionally solidify in space as perceptibly Bi-rich, off-
eutectic compositions, with a Bi solid solution phase enriched in Mn.
Decreased MnBi volume fraction and Bi-rich type macrosegregation were observed
experimentally, and will be commented on later. Of course, any low-gravity
induced phase diagram changes will also be reflected in solidification of
nominal off-eutectic compositions.

The total undercooling of the eutectic interface in any of the numerous
analyses is a function of interface velocity, V, (for example, Ref. 17):

$$\Delta T = K_1 V \lambda + \frac{K_2}{\lambda} + \Delta T(V) \tag{2}$$

where K_1 and K_2 are constants and $\Delta T(V)$ is a kinetic undercooling term. The
first term is the constitutional undercooling and the second term is the
curvature undercooling due to the Gibbs-Thompson effect. For regular
eutectics which grow with a minimum undercooling this reduces to $\Delta T =
2(K_3 K_4)^{1/2} V^{1/2}$, with $\lambda^2 V = K_4/K_3$. An argument previously suggested to explain
the SPAR Bi/MnBi eutectic experiments (Ref. 4) notes that temperature
fluctuations in the melt, caused by turbulent convection when the thermal
gradient exceeds a critical value, may induce nonsteady-state interface
motion. It was argued that if the eutectic nucleation or branching proceeds
more slowly than MnBi rod termination, then the mean interface growth velocity
might decrease in the presence of this supercritical convection. By the above
equations it can be seen that if this supercritical convection is achieved at
earth gravity, then λ will be larger and ΔT will be smaller in earth gravity
compared to low gravity. This will also account for the observed phenomena in
the previous SPAR experiment. This explanation, however, now seems somewhat
less likely with the finding that the MnBi rod spacing was able to adapt more
rapidly than the freezing rate could be changed in a recent experiment (Ref.
7). Therefore, in the present and upcoming experiments, we would particularly
like to test the idea of an increased undercooling in low gravity which
modifies the phase diagram in the Bi/MnBi system.

7

EXPERIMENTAL PROCEDURE

SAMPLE PREPARATION & DIRECTIONAL SOLIDIFICATION PROCESSING

Off-eutectic Bi/MnBi ingots of 0.90 and 0.49 w/o Mn were made using commercially pure Mn (99.9 w/o) and high purity Bi (99.999 w/o) by induction heating in evacuated and sealed 4 mm inner-diameter quartz tubes and quenching by turning off the coil power. Ingot lengths were about 2.5 cm. A 1/4 mm diameter hole was drilled about 1 cm deep to place one 0.004 cm bead-diameter chromel-alumel thermocouple in each ingot. Each starting ingot was encapsulated in an evacuated 4 mm inner diameter quartz ampoule as described previously (Ref. 2 and 3).

Samples were directionally solidified using the Bridgman-Stockbarger technique in furnace assemblies built by General Electric (Ref. 18). The same unit with identical parameters was used for both low-gravity and earth-gravity comparison solidifications. The apparatus, referred to as the ADSS, Automatic Directional Solidification System, consisted of four furnace assemblies mounted symmetrically with their longitudinal axes parallel. Opposite assembly pairs moved in unison and in the opposite direction from the other furnace pair to keep total apparatus momentum equal to zero. On the ground, this feature was used to solidify compositions parallel and antiparallel to the gravity vector in order to create differing amounts of convection in the melt. For both flight and ground-based solidification, furnaces No. 1 and 2 contained samples No. 1 and 2 of composition 0.90 w/o Mn and furnaces No. 3 and 4 contained samples No. 3 and 4 of composition 0.49 w/o Mn. On the ground, furnaces No. 1 and 3 solidified samples up (antiparallel to the gravity vector) and furnaces No. 2 and 4 solidified samples down (parallel to the gravity vector).

The furnace assemblies were capable of producing a planar solidification interface near the equilibrium solidification temperature of 265°C with gradients of 20 to about 150°C/cm and furnace velocities of 0.3 to 50 cm/h. For this experiment, nominal values of 140°C/cm and 11 cm/h were chosen. The furnace translated along the stationary tubular quartz sample ampoule

described above. A description of the methods of monitoring the furnace and sample temperatures and velocities during solidification has been given previously (Ref. 19).

EARTH-GRAVITY & FLIGHT EXPERIMENTS

Off-eutectic Bi/MnBi samples were directionally solidified in low gravity aboard the SPAR X flight on June 17, 1983. Prior to the launch, persistent problems with ground-based tests using the flight furnace assembly extended over several months, preventing a flight-comparison, ground-based solidification experiment (referred to as the All-Systems Test) from being run prior to the launch. A post-launch solidification experiment with SPAR X processing parameters was performed on the ground at Marshall Space Flight Center for comparison to the low-gravity results. One sample of each composition was solidified up and one down with respect to the gravity vector.

The SPAR X flight experiment began on the ground with a 30 min furnace warmup, reduced from the originally desired 120 min by the same prelaunch problems of persistently erratic furnace motion. Before previous SPAR launches using this assembly, cleaning and relubrication of moving parts had alleviated any problems with erratic furnace velocity. This same problem was noted before the SPAR X launch but was found to become critical when the furnace was hot. Prelaunch experiments suggested that reducing the warmup time from 120 to 30 min should be adequate for the furnaces to reach the desired maximum temperature and would allow the furnace motion to become more regular. It is noted here that this problem has been repaired for the space shuttle apparatus by the use of low thermal expansion, metal-impregnated nylon drive bushings. After launch, directional solidification began 38 s after $10^{-4}g_e$ was obtained. The solidification time interval in low gravity was 265 s (approximately 0.81 cm furnace travel) and furnaces were stopped after 604 s of total furnace travel time.

Ground-based sample No. 2 solidified in a fashion to be described later which was inadequate for study. Therefore, a replacement sample was solidified in our laboratories at Grumman Aerospace Corporation using a furnace built by GE as a prototype to the ADSS flight furnaces and conditions which were nominally identical to those of the flight.

9

POST-SOLIDIFICATION SAMPLE HANDLING

Each SPAR X ground-based and flight sample was first polished shallowly lengthwise to inspect for solidification irregularities and dendritic growth. Samples were scribed on one side for identification and were then partitioned into pieces about 0.3 cm long by a low speed cutoff wheel with a 0.035 cm thick diamond-impregnated copper blade. This resulted in about 8 sections per sample. Sections were labeled according to flight or ground-based processed, furnace number, and position in sample, starting with the letter "A" at the first solidified end of the sample. Each section was cleaned, weighed, and its length measured. Sections were then ready for mounting for measurement of their magnetization.

Sections were prepared for microstructural examination by polishing the cross-sectional surface of each section away from the first solidified end (except for the last section). Sections were mounted in a cold plastic mounting compound, polished in a sequence ending with 0.05 μm Al_2O_3, and etched lightly with a 10% solution of acetic acid in water. A morphological analysis was then conducted for each sample. A few selected sections were broken out of mounts and then heat treated at 250°C for 36-48 h, and reexamined magnetically and microstructurally. All sections in plastic mounts were given a light refinishing on 600 paper to remove the etched surface layer and were then examined by X-ray fluorescence. In addition, two sections were broken out of their plastic mounts, cleaned in acetone, and destructively chemically analyzed.
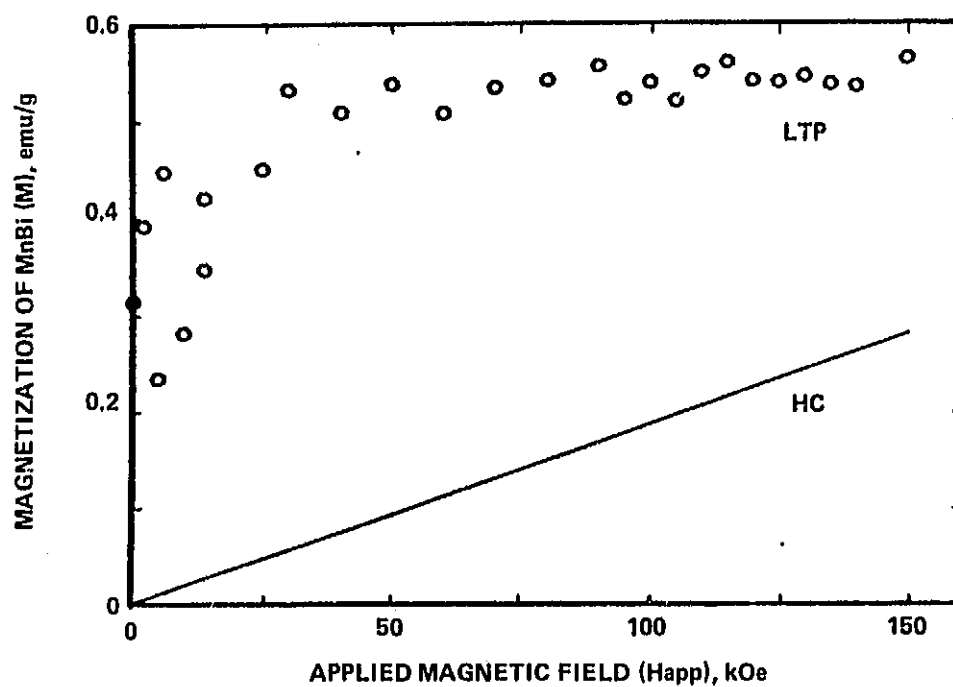
MAGNETIC PROPERTY, MORPHOLOGICAL, CHEMICAL & THERMAL ANALYSIS

Magnetic properties were determined for each section from the measured magnetizations, which were measured as a function of the applied magnetic field at the Francis Bitter National Magnet Laboratory. Measurements were made parallel to the aligned microstructure at room temperature in applied fields typically up to 150 kOe using a low frequency vibrating-sample magnetometer. At room temperature three magnetic phases have been shown previously to coexist in directionally solidified Bi/MnBi (Ref. 2, 5 and 20). The matrix, Bi solid solution, is diamagnetic with a (negative) susceptibility which is weakly dependent on Mn concentration. The expected

10

equilibrium MnBi phase is strongly ferromagnetic and is referred to as the low temperature phase (LTP). A new, second MnBi phase, referred to as the high coercivity phase (HC) due to its large intrinsic coercivity at cryogenic temperatures where it is ferromagnetic, was found to be metastable and paramagnetic at room temperature. These three phases are magnetically additive at room temperature which allows the separation of the effects of each phase. The ferromagnetic character of the equilibrium MnBi phase can provide a measure of the effect of solidification processing on MnBi rod size and alignment. For example, as the rod diameter approaches the magnetic domain size, the resistance to demagnetization or intrinsic coercivity of a sample containing only LTP MnBi approaches the theoretical maximum of 35 kOe (Ref. 4). Also, dendritic samples will exhibit a decreased remanent magnetization and intrinsic coercivity. In previous work, the separate hysteresis curves of the LTP and HC phases at 77 K were used to determine the amount of each magnetic phase and hence the total volume fraction of MnBi (Ref. 21) or the composition of samples in an off-eutectic experiment (Ref. 1). Using the parameters for the magnetic phases found in this previous work and the assumption of 0.11 w/o Mn in the Bi solid solution, the magnetization at room temperature has been used to determine magnetic phase and chemical composition of each sample in this study. This involved an iterative approach in which the volume fraction MnBi was first calculated. A first approximation of the amount of Bi solid solution was then returned with its diamagnetic contribution into the calculation of the volume fraction MnBi, the process being repeated until self-consistency was achieved. Figure 2 illustrates the separation of the magnetic MnBi phases from the magnetization data for flight sample No. 2 section A. Figure 2(a) shows the magnetization data normalized to sample weight, including a linear least squares fit to the data between 80 and 150 kOe where the hysteresis curve saturates. This fit was used to obtain the representation of the magnetization due to LTP and HC phases for this section as shown in Fig. 2(b). Small section size meant that significant noise was present in the magnetization data which resulted in a typical uncertainty of ±5% in Mn composition values.

11

0.8

0.6

0.4

0.2

0

MAGNETIZATION Bi/MnBi (M), emu/g

0   50   100   150

APPLIED MAGNETIC FIELD (Happ), kOe
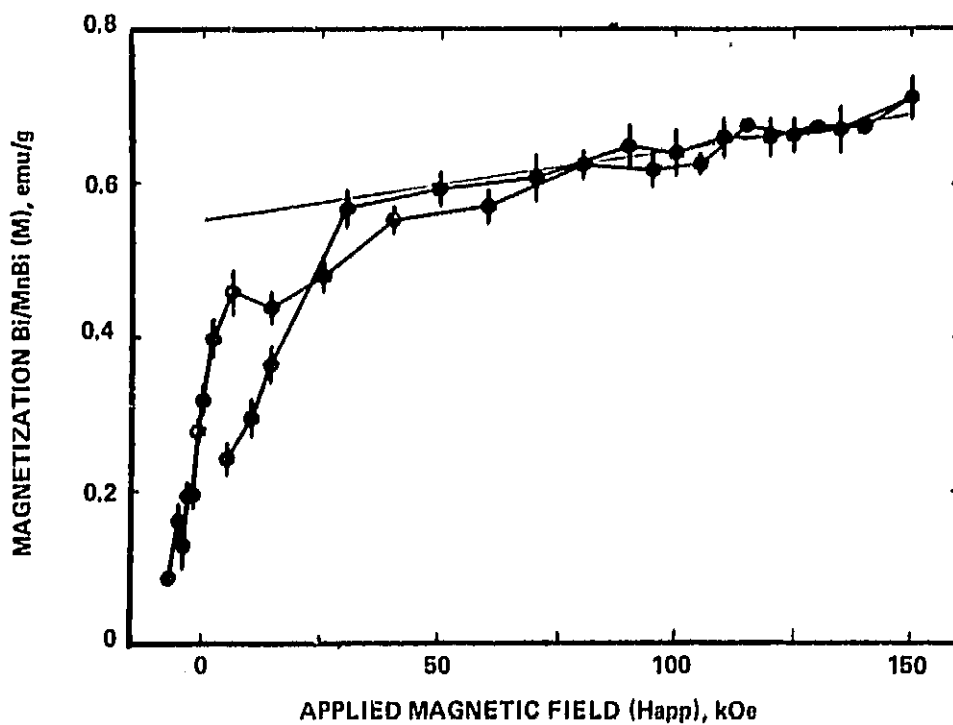
a. Data With Straight Line Representing L.S. Fit to Data Between About 80 & 150 kOe

0.6

0.4

0.2

0

MAGNETIZATION OF MnBi (M), emu/g

LTP

HC

0   50   100   150

APPLIED MAGNETIC FIELD (Happ), kOe

b. Deconvolution of Magnetization into MnBi LTP & HC Phases After Elimination of Bi Solid Solution Contribution

1330-002(T)

Fig. 2   Room Temperature Magnetization of Flight Sample No. 2 Section A

12

Microstructural and quantitative MnBi rod diameter and interrod spacing analyses were performed using a computer-aided Leitz particle analysis system. Approximately 2000 rods in 10 to 20 different views of a section surface were analyzed directly from a live video camera image, which allowed great control over focus, contrast, magnification, and lighting adjustments to produce the most representative image of the surface. Mean rod diameters, $<d>$, mean interrod spacings, $<\lambda>$, and standard deviations of the distributions were determined by either of two techniques. Histograms of the variable could be smoothed by hand and the mean extracted with half width at half maximum taken as the standard deviation. A more analytical approach was to fit a histogram with a modified Poisson distribution by minimizing χ^2, and to use the modified Poisson parameters to obtain the mean and standard deviation. In addition, MnBi volume fraction and Mn concentration (assuming 0.11 w/o in solid solution) were calculated directly from the camera images by the computer.

In order to check the accuracy of the Mn concentration values from magnetic and optical measurements and, in addition, to assess the correctness of the assumed value of the Mn concentration in Bi solid solution, X-ray fluorescence determinations of the total Mn concentrations near the surfaces of most of the sections of the samples were made. Measurements were performed by Fairfield Testing/LabTech, Inc. using Cu radiation. Three pieces each, of five Bi/MnBi cast ingots, of compositions 0.0, 0.4, 0.6, 0.7, and 0.9 w/o Mn in Bi were used to calibrate the Mn/Bi count ratios. The precision for these determinations was about 0.1 w/o Mn.

As the most reliable but destructive technique for measuring the bulk total Mn concentration of a Bi/MnBi section, chemical spectrophotometric absorbance (CSA) was used for a limited number of samples (Ref. 22). This technique had a sensitivity of ± 0.05 w/o Mn.

Thermal measurements from the in situ thermocouple in each sample and two reference block thermistors were made as functions of elapsed solidification time at a rate of about one reading per second for each furnace assembly. These measurements were transmitted via telemetry and recorded both in digital

13

and analog form. It was convenient to digitize the analog traces via a digitizing pad connected to a computer. Voltages representing the resistance of the thermistors were converted to temperatures (Ref. 18) with a fourth-order polynomial and subsequently these temperatures were converted to equivalent K-type reference junction voltages by an eighth-order polynominal representation of the μV-T curve (Ref. 23). These voltages were added to the thermocouple voltages as a function of the elapsed time and the summed voltages were converted to sample temperature profiles with a fourth-order polynomial (Ref. 24). Due to a lack of point-to-point grounding in the ADSS apparatus, resolution of the in situ thermocouple measurements was limited to ± 0.07 mV (± 1.9°C).

RESULTS

LOW-GRAVITY EXPERIMENT - GENERAL OBSERVATIONS

On June 17, 1983 SPAR X was successfully launched from White Sands
Missile Range and the payload was recovered later the same day. The ampoules
were promptly removed and reached Grumman on June 21, 1983.

The Bi/MnBi off-eutectic samples in all ampoules were completely
intact. As is shown in Fig. 3, the end of each glass ampoule opposite from
the thermocouple was broken off. The unoxidized state of each sample
indicated that the breakage occurred when the rocket hit the desert floor.

X-ray radiographs of the flight ampoules are shown in Fig. 4 and detail
exact shapes of samples and slight leakby, but reveal no internal porosity.
Photographs of the removed samples, with thermocouples and a graphite plug in
place, are shown in Fig. 5. Sample No. 1 separated into two distinct pieces
during its molten period due to the free volume created by leakby and
contraction on melting. Sample No. 2 separated into two pieces about 3 mm
from the first-solidified end of the sample, but the two pieces remained
touching. Sample No. 3 looked perfect in form, as did sample No. 4, except
the latter sample was fractured into two pieces at some time following
solidification. This did not affect analysis of sample No. 4.

Evaluation of the telemetry data indicates that coolant pumps were
functioning adequately to maintain the coolant temperatures within
requirements, and reference transistors, cold junction thermistors, furnace
thermocouples, and furnace assemblies appeared to operate properly. An
occasional abrupt jump in the sample temperatures was evident in the data and
was smoothed in the temperature plotting when it was believed to be too abrupt
to be real. A more serious problem was the fact that the sample temperatures
appeared to never reach the solidification temperature within the furnace
travel time (Fig. 6), despite the fact that the thermocouple tip was located
only 1 cm into the sample and that the end of the sample was believed to have
been placed at the face of the chill block. There are three possible
explanations for this problem. One is that the telemetry data drifted from
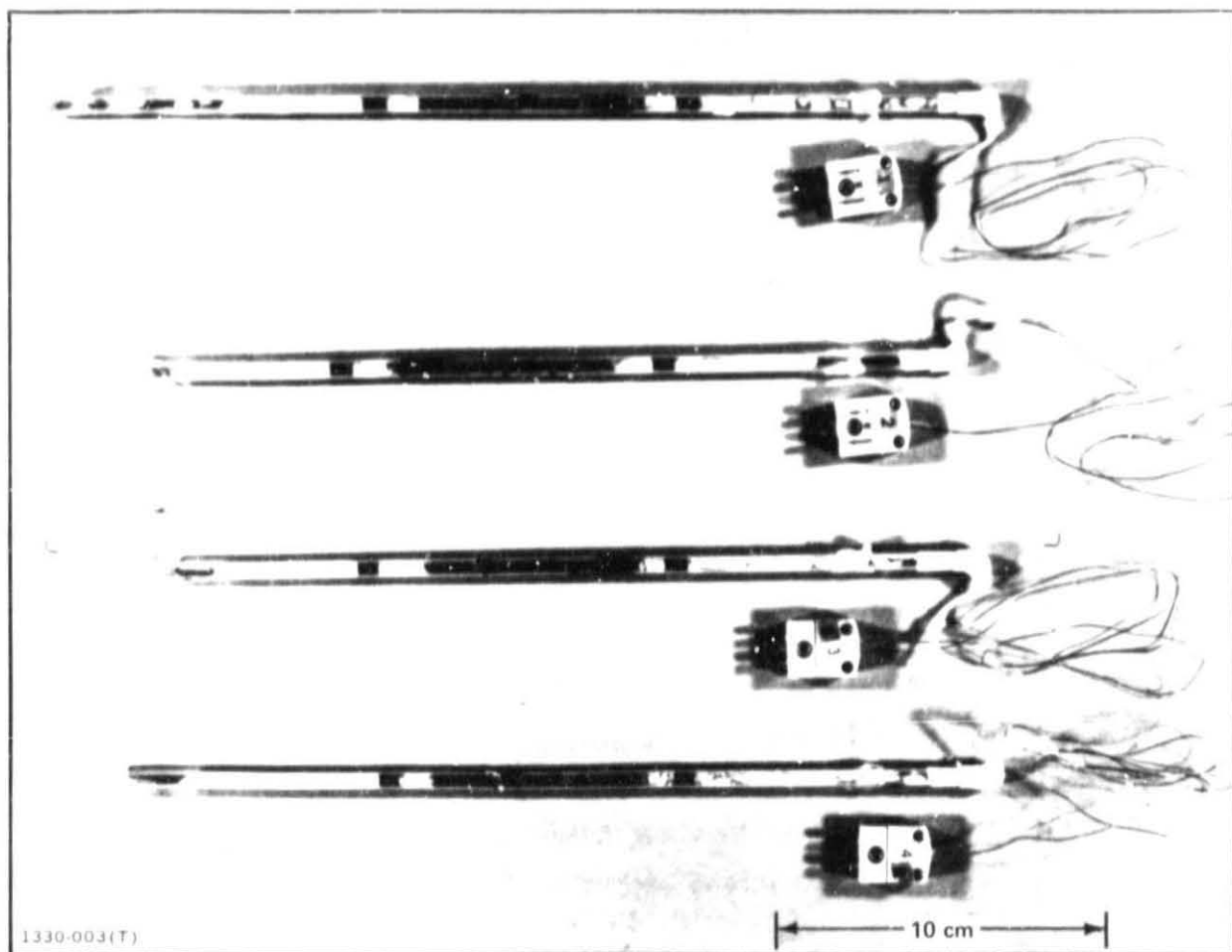the true temperature values as the assembly and electronics temperature

15

Fig. 3 SPAR X Flight Ampoules as Received After the Low-Gravity Flight Experiment
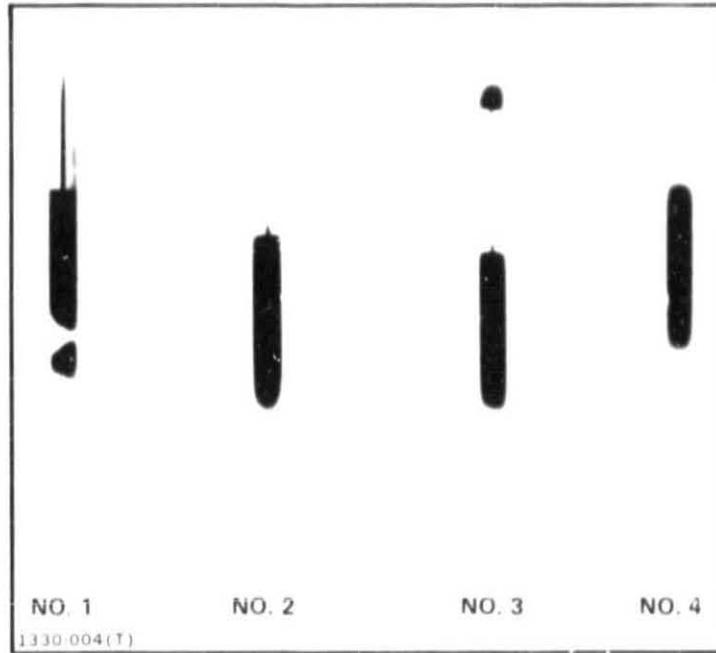
16

NO. 1   NO. 2   NO. 3   NO. 4

1330-004(T)
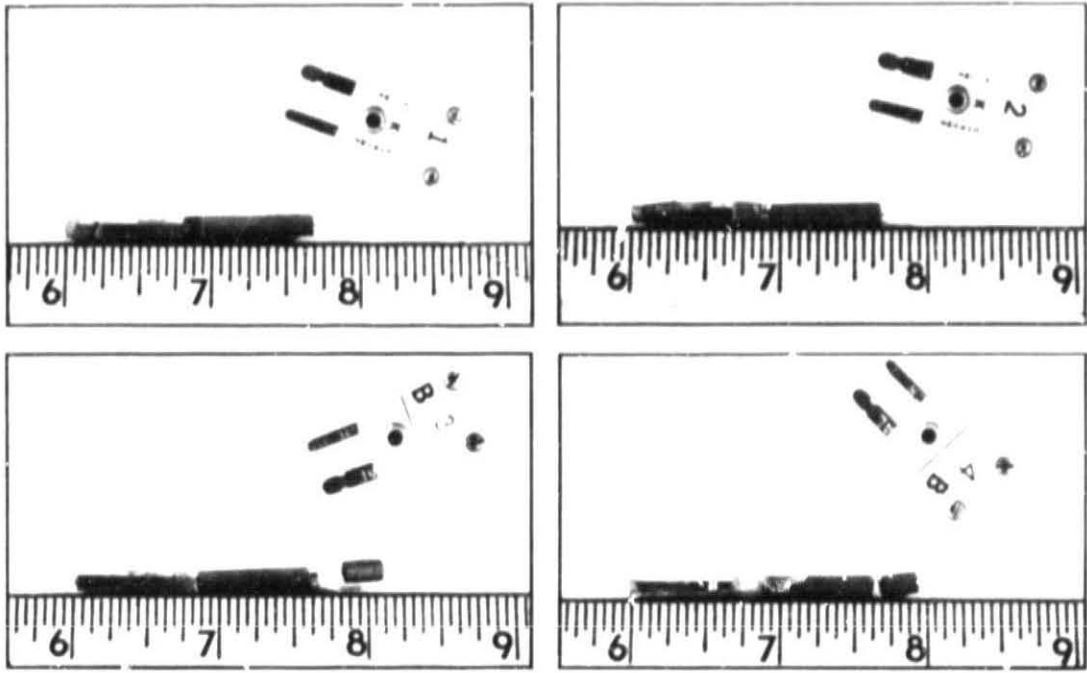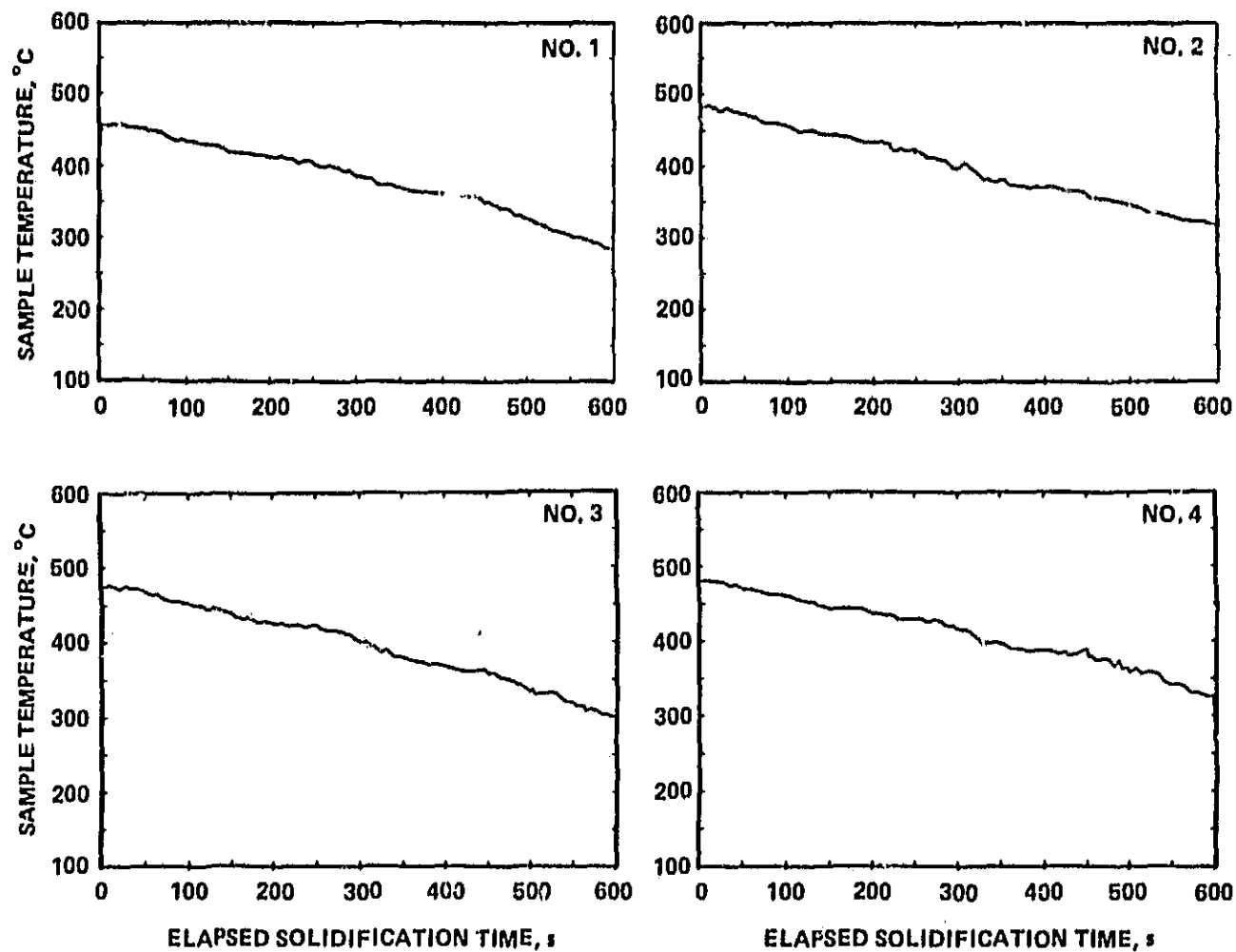
Fig. 4   X-Ray Radiographs of Flight Samples
Before Removal from Ampoules

1330 005(T)

Fig. 5 Photographs of Flight Samples After Removal From Ampoules

Fig. 6 Temperature Profiles of Flight Samples No. 1-4 at Thermocouples

1330-006(T)

19

increased. This is supported by the alignment of the MnBi rods parallel to the sample axis and the apparent directional solidification to the last solidified end of each sample. The temperature profiles of the post-flight ground-based comparison experiments, shown in Fig. 7, provide additional information about this problem. A distinct break in the temperature profile of sample No. 4 at about 310 s corresponds well to the expected time for the solidification front to reach the thermocouple tip. In addition, no break in this profile is visible near 265°C where the gradient should change rapidly to the value in the solid. A second possible explanation of the temperature profiles assumes the data is correct and the end of each sample was positioned incorrectly by about 1 cm from the initial position of the solidification front near the chill block. The third possibility is that, again, the data is correct, but each sample was positioned near the chill block and at these high furnace temperatures the initial position of the freezing isotherm was about 1 cm within the chill block. Since it is unlikely that the freezing isotherm could be moved a distance of 1 cm by a relatively small increase in temperature, this last suggestion is dismissed. Given the difficulty of choosing between the two remaining explanations, the problem is left to be resolved later and the analysis of the experiment will continue cautiously.

In spite of the last moment prelaunch furnace velocity difficulties, the velocity telemetry data indicated, within the noise signal, stable furnace motion except for furnace No. 2 the velocity profile of which is shown in Fig. 8. The average speeds for furnaces No. 1, 2, 3, and 4 were 11.1, 11.4, 10.3, and 11.5 cm/h respectively with a noise level of ± 0.7 cm/h, as seen in Table 1.

All flight samples and most ground-based samples had microstructural banding in the first solidified portions of the samples. A typical example is seen in Fig. 9. The extent of banding ranged from less than 0.2 cm in the first piece of flight sample No. 2 to about 1.5 cm in the ground-based sample No. 4, with most samples in the lower part of the range. The most probable cause of this is slightly unsteady furnace motion, with velocity changes within the noise signal of the velocity data.

The furnace thermocouples showed an unusually wide spread in hot zone

20
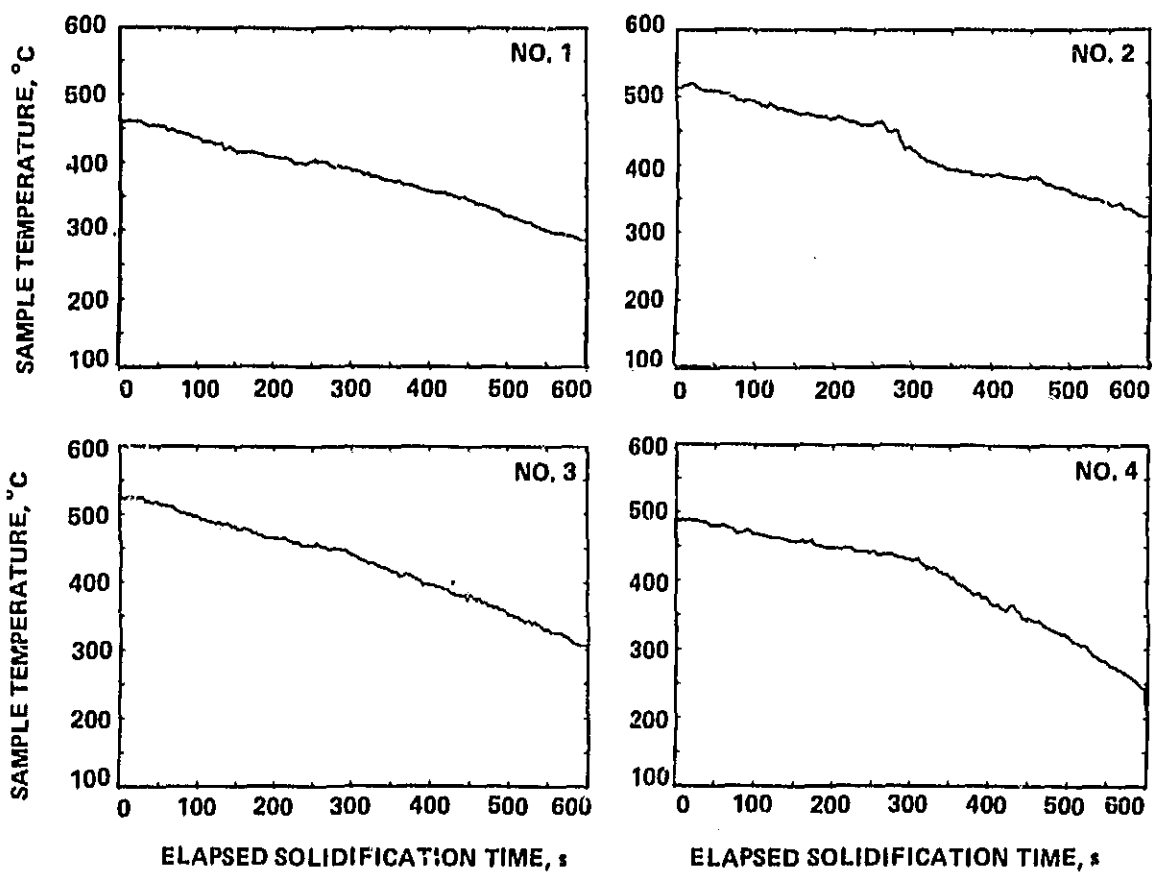
1330-007(T)

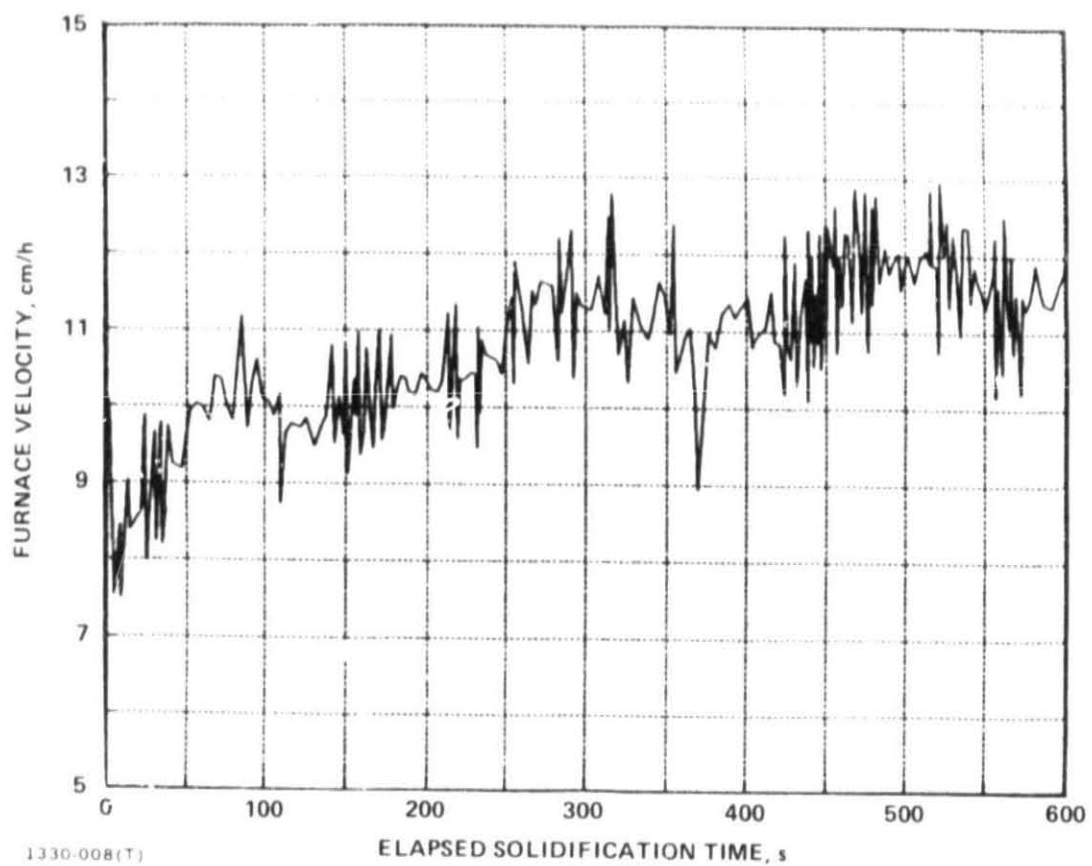Fig. 7 Temperature Profiles of Ground-Based Comparison Samples No. 1-4 at Thermocouples

21

Fig. 8 Velocity Profile of Flight Furnace No. 2

1330-008(T)

Table 1 Comparison of Thermal Properties for Samples Grown During SPAR X & Ground-Based Comparison Experiments. Velocities are Average & Thermal Measurements were Taken at 1 cm Furnace Travel

EXPERIMENTAL MEASUREMENT OR CONDITION	SPAR X FLIGHT (10^{-4} g) FURNACE ASSEMBLY NO.				GROUND-BASED COMPARISON FURNACE ASSEMBLY NO.			
	1	2	3	4	1	2	3	4
NOMINAL INITIAL BULK COMPOSITION, w/o Mn	0.90		0.49		0.90		0.49	
SOLIDIFICATION GEOMETRY	–	–	–	–	UP	DOWN	UP	DOWN
FURNACE VELOCITY, $\times 10^{-3}$ cm/s	3.08 ±0.3	3.17 ±0.3	2.86 ±.03	3.19 ±0.3	3.25 ±0.3	3.11 ±0.3	2.78 ·0.3	3.19 ·0.3
FURNACE HOT ZONE TEMP, °C	481 ±3	521 ±3	587 ±3	583 ±3	506 ·3	544 ·3	608 ·3	584 ·3
FURNACE CHILL BLOCK TEMP, °C	38 ±1	38 ±1	38 ±1	38 ±1	36 ·1	36 ±1	36 ·1	36 ·1

1330-017(T)

23

GROWTH DIRECTION |←— 500 μm —→|

1330-009(T)

Fig. 9 Microstructural Banding in Flight Sample
No. 4, Longitudinal View

24

temperatures, as seen in Table 1. Also, the higher furnace hot zone temperatures in low gravity observed previously (Ref. 4) were not recorded in this work. The causes of these observations, if real, are unknown.

NORMAL-GRAVITY OBSERVATIONS

Ground-based comparison samples were solidified at Marshall Space Flight Center after the SPAR X launch, with the same furnace system and nominal processing parameters as for the flight experiment. These samples were received at Grumman on July 5, 1983. Table 1 lists the directional solidification conditions of these experiments and Fig. 7, which shows the thermal profiles of the solidifications, indicates the same problem for the ground-based experiment as occurred in the flight experiment thermal profile.

Sample No. 1 was observed to have separated from the graphite plug by about 0.5 cm at the last-solidified end. Sample No. 2 was pulled into two pieces in the liquid state. A second sample No. 2 was processed later at MSFC with identical results. Therefore, a sample of identical composition was solidified at Grumman with the same nominal processing parameters to replace this particular sample. Samples No. 3 and 4 were well formed in outer appearance, although during removal from the ampoule, sample No. 4 broke into two pieces, which did not impact the analysis.

Particular sections of samples were annealed in an evacuated quartz tube at 250°C for 36-48 h to simplify the magnetic analysis for those sections to that involving only the two equilibrium phases. The effect of heat treatment on the aligned-growth microstructures of samples solidified in this experiment is visible in Fig. 10. Chevron and triangular rod cross sections annealed to circular cross sections in every sample examined in this study. This finding is in contrast to previous work (Ref. 25) which did not find rod shape changes. Preliminary quantitative analysis of average rod areas and interrod spacings of annealed sections suggests that "coarsening" of rods did not take place and that the average rod area remained unchanged as the rod shape changed. One interesting possibility is that interfacial energies of the HC phase are lower than those of the LTP. This new finding of a shape change will be studied further at a later date.
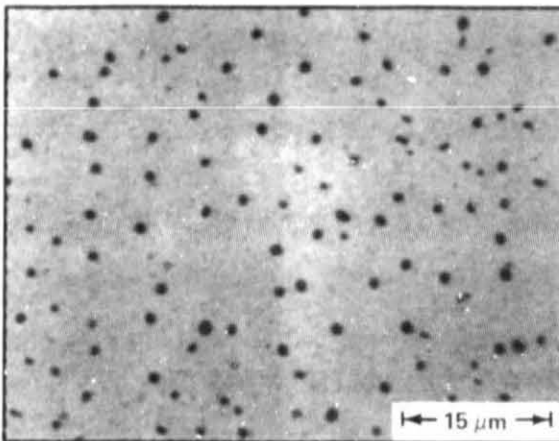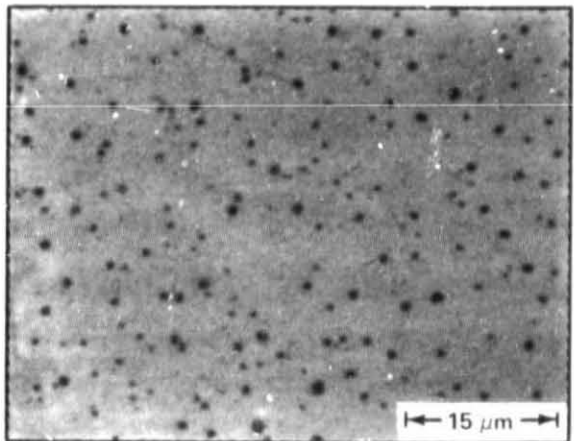
25
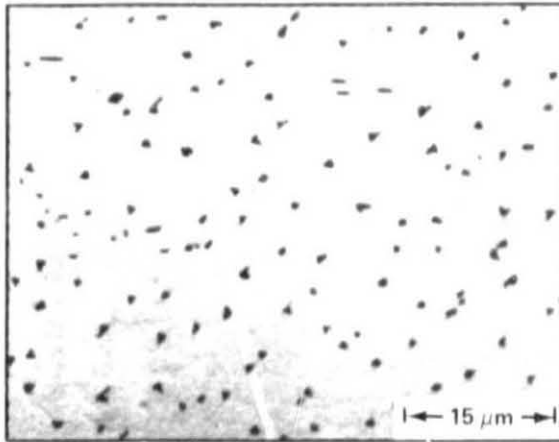
a. Ground-Based Sample No. 3, Fraction
   Solidified = 0.43 Pre-anneal
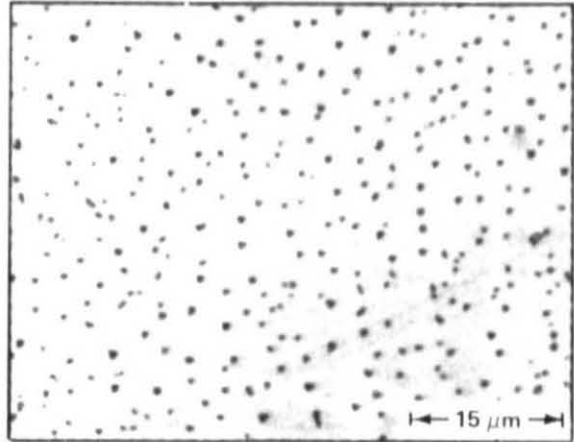
c. Flight Sample No. 3, Fraction
   Solidified = 0.19, Pre-anneal

b. Same as (a), but Post-anneal

d. Same as (c), but Post-anneal

1330-010(T)

Fig. 10 Comparison of Microstructures Transverse to Solidification Direction
in the As-Grown State & After Heat Treatment at 250°C for 36-48 h

26

Sections of the ground-based comparison samples were examined microstructurally on cross-sectional faces to determine the morphology of the MnBi phase on each face. Magnetic measurements and X-ray fluorescence measurements were made on sample sections to determine Mn content of the solid bulk and local cross-sectional surface, respectively. We begin to examine the results with sample No. 3. Sample No. 3 was Bi-rich and contained a few small areas of Bi solid solution cells or dendrites throughout most of the length of the sample, the remainder of the volume being an aligned MnBi rod-Bi solid solution matrix structure. Although this sample contained dendrites, a quantitative fit of the longitudinal macrosegregation for sample No. 3 was attempted and illustrated in Fig. 11. As described in the background section of this report, such a quantitative description of macrosegregation for directional plane-front, off-eutectic composite growth, including the effect of convection, has been developed by Verhoeven and Homer (Ref. 9) using a Burton-Prim-Slichter type stagnant film analysis. The average solid composition in a/o Mn, C_S, as a function of fraction solidified, f, is given by

$$C_S = C_E - \frac{C_E - C_0}{1-\exp{(-p\delta)}} \ (1-f)^{-1/(1-\exp{(p\delta)})} \qquad (3)$$

where C_E is the eutectic composition, C_0 is the starting composition, p is the inverse of the Stefan length or solute boundary layer distance, and δ is the characteristic stagnant film length. This form of their equation neglects thermotransport and is used here because of the relatively high growth rate for this experiment. Previously, it was reported for the Bi/MnBi off-eutectic system that this equation fit the macrosegregation data even when the growth was partially dendritic (Ref. 1). This might be because in this system with the processing conditions used, the growth may possibly still proceed with a macroscopically planar solidification isotherm. The relatively few dendrites may perturb the macrosegregation only slightly. In addition, the above equation has a very general Scheil-equation form so that although pδ may not be the proper exponential parameter, the equation still fits the data for this experiment. For the cases here, where a substantial length of the sample contained dendrites or cells, KV is substituted for pδ in Eq (3), where K is the effective distribution coefficient. Figure 11 shows a best fit to the

27

O   BULK COMPOSITION FROM MAGNETICS
X   SURFACE COMPOSITION FROM X-RAY FLUORESCENCE
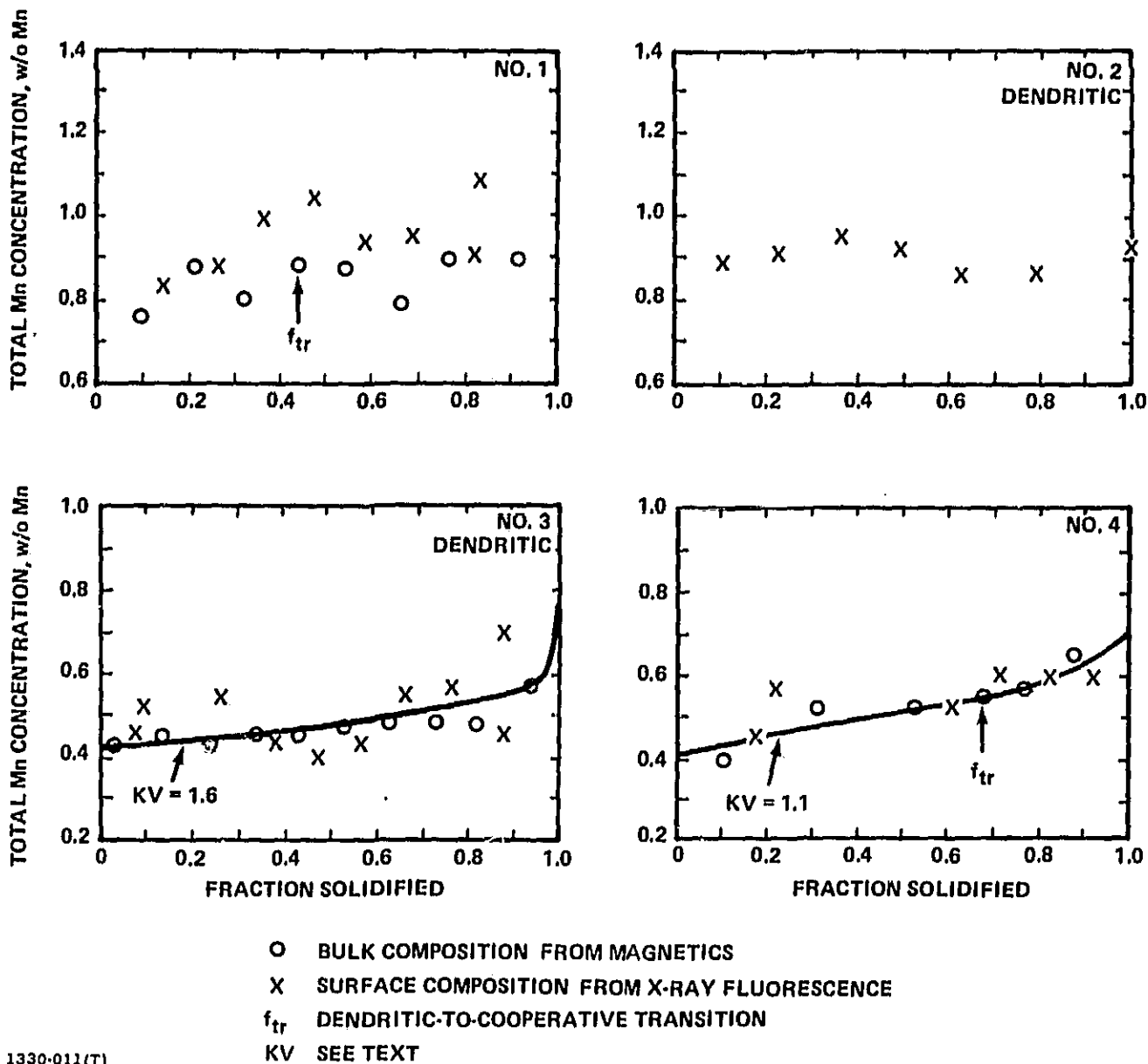f_{tr} DENDRITIC-TO-COOPERATIVE TRANSITION
KV   SEE TEXT

1330-011(T)

Fig. 11 Total Mn Composition vs Fraction Solidified for Ground-Based Samples

macrosegregation data of sample No. 3, where KV = 1.6. Sample No. 4 was also Bi-rich and contained dendrites or cells up to f_{tr} = 0.67 where the morphology became completely aligned (see Fig. 12). Results of quantitative analysis of the aligned microstructure of a section of sample No. 4 are shown in Table 2. It is noted here that the normal-gravity equilibrium value of 0.11 w/o Mn in the Bi solid solution was assumed for the calculations of composition. Figure 11 displays the macrosegregation of sample No. 4 and includes a fit of Eq (3) with KV = 1.1.

Sample No. 1 was Mn-rich and underwent a dendritic-to-cooperative transition at f_{tr} = 0.44. Table 2 lists the quantitative microstructural analysis results for two cooperative sections of sample No. 1. Solutal macrosegregation (Fig. 11) appears to be minimal, although there is wide scatter in the compositional results, due in part to the very small size of the analyzed sections. Minimal macrosegregation implies in this case that KV > 1.6. In initial ground-based studies of growth up of Mn-rich compositions, Stokes flow was observed - that is, floatation of MnBi dendrites to the top of the melt, causing gross macrosegregation disturbances. This was particularly a problem with sample composition greater than 0.9 w/o Mn, and appears to have been successfully minimized in sample No. 1. Sample No. 2, as discussed previously, is a Grumman-solidified sample. The entire sample was scattered with MnBi dendrites, although Fig. 11 shows that, similarly to sample No. 1, no macrosegregation of Mn appears to have taken place, again implying KV > 1.6.

The percentage of the MnBi which is in the HC phase for the ground-based samples No. 1, 3 and 4 is shown in Fig. 13. Results generally fall in the 60-70% range and show only very weak dependence on the fraction solidified, f, or the Mn composition. HC phase percentages are this high because of the moderately high solidification velocity and the high gradient (see Ref. 4).
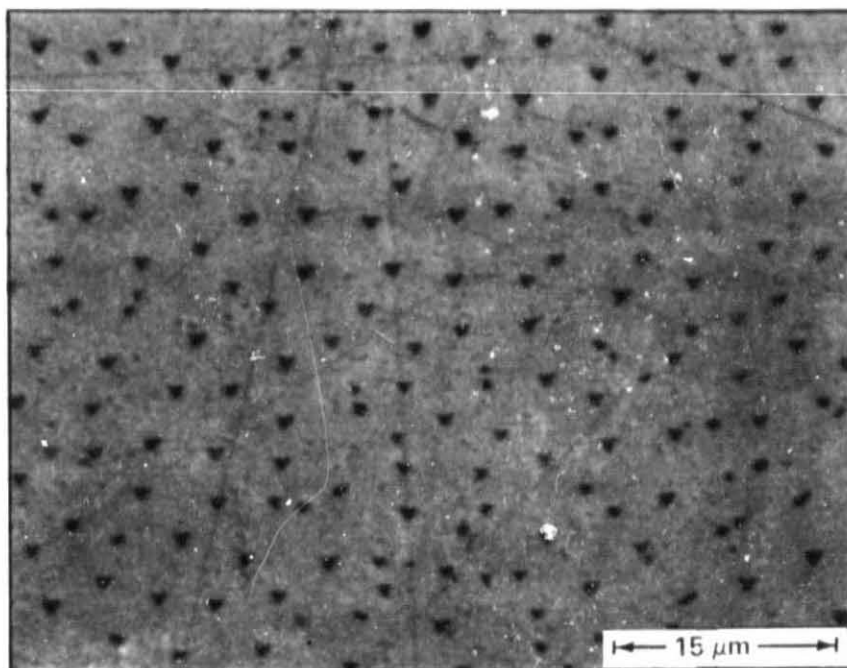
FLIGHT RESULTS & NORMAL-GRAVITY PROPERTY COMPARISON

Flight samples No. 3, 4, and 1 were dendritic in the initial (proposed) low-$\bar{g}$ portions of the samples. Figure 14 shows resultant macrosegregation and Fig. 15 the fraction MnBi in the HC phase for these samples. Within the

29

|←— 200 μm —→|
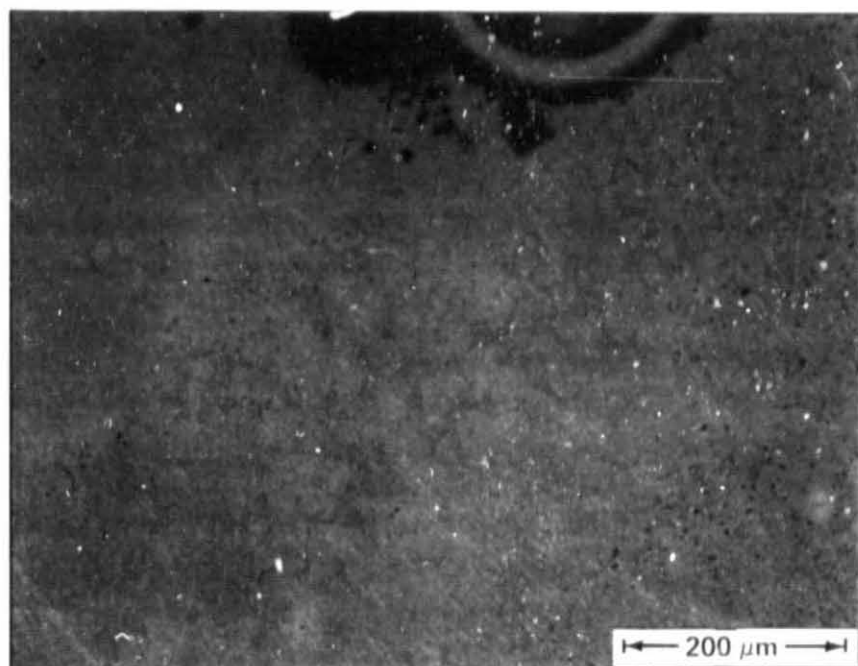
Dendrites Near Thermocouple at f = 0.19

|←— 15 μm —→|

Cooperative Structure at f = 0.75

1330-012(T)

Fig. 12 Microstructures Representative of Ground-Based Sample No. 4.
Dendritic-to-Cooperative Transition is at f_{tr} = 0.67

Table 2 Results of Quantitative Analysis of Cooperative Microstructures from Sections of Samples Grown During Ground-Based Comparison and SPAR X Flight Experiments

SAMPLE NO.	f	$\langle d \rangle$, ±0.05 μm	σ, μm	$\langle \lambda \rangle$, ±0.3 μm	σ, μm	c_{Mn}, w/o	c^*_{Mn}, w/o
GROUND-BASED							
4	0.916	0.62	0.16	2.9	1.1	0.62	0.64
1	0.468	0.93	0.16	3.1	1.0	1.10	0.90
1	0.797	0.65	0.18	2.5	1.1	0.81	0.90
FLIGHT							
3 (ANNEALED)	0.980	0.77	0.17	3.2	1.1	0.74	0.72
4	0.840	0.69	0.18	3.3	1.4	0.59	0.54
2	0.195	0.50	0.18	2.3	1.1	0.61	0.62
2	0.445	0.77	0.19	3.2	1.4	0.69	0.72

c_{Mn} = Mn CONCENTRATION DETERMINED BY MICROSTRUCTURAL ANALYSIS

c^*_{Mn} = BULK Mn CONCENTRATION EXTRAPOLATED FROM MAGNETIC MEASUREMENT DETERMINATIONS
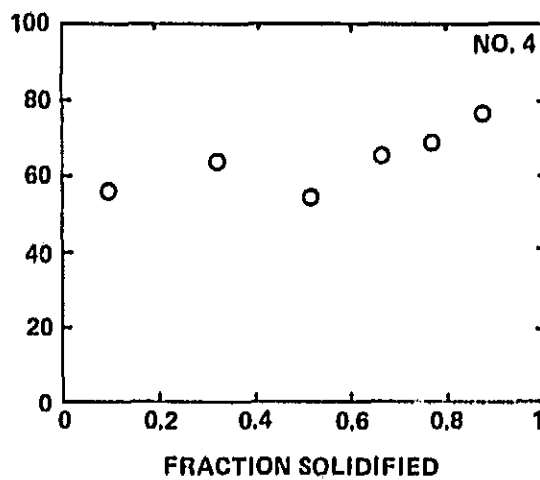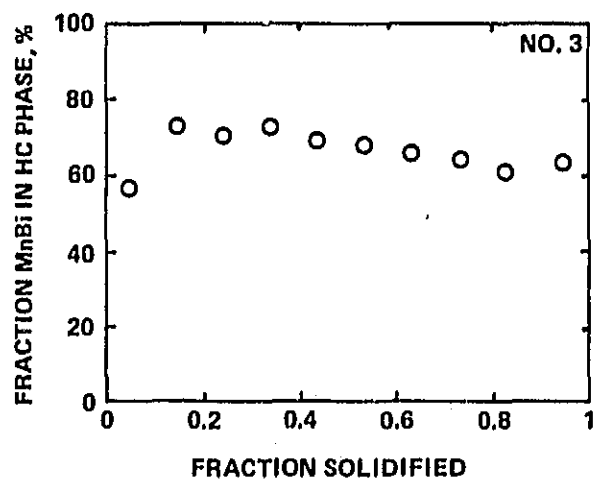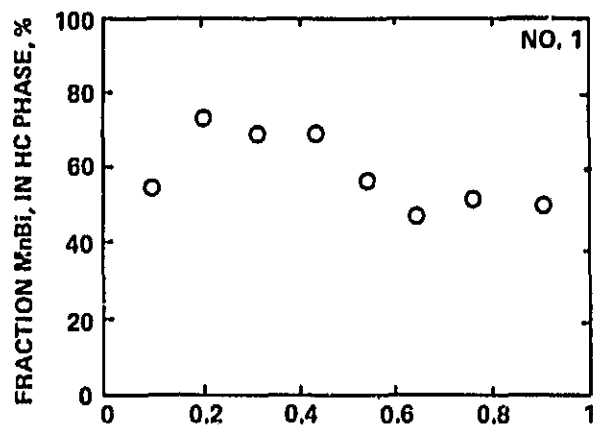
1330-018(T)

Fig. 13 Fraction of MnBi in the HC Phase vs Fraction Solidified for Ground-Based Samples

32

Fig. 14 Total Mn Composition vs Fraction Solidified for Flight Samples

O   BULK COMPOSITION FROM MAGNETICS
X   SURFACE COMPOSITION FROM X-RAY FLUORESCENCE
▲   BULK COMPOSITION FROM CSA
f_{tr} DENDRITIC-TO-COOPERATIVE TRANSITION

1330-014(T)

33
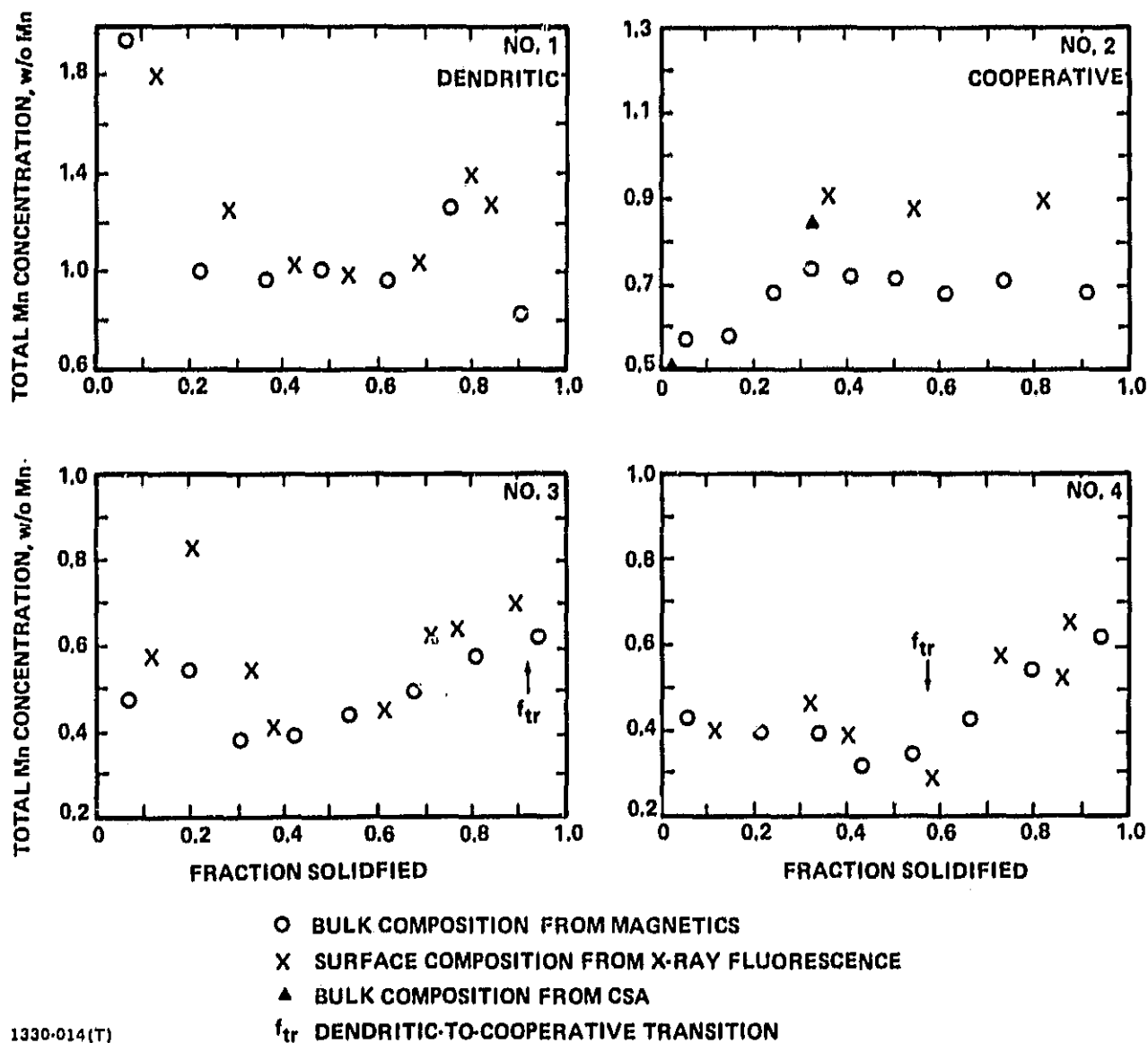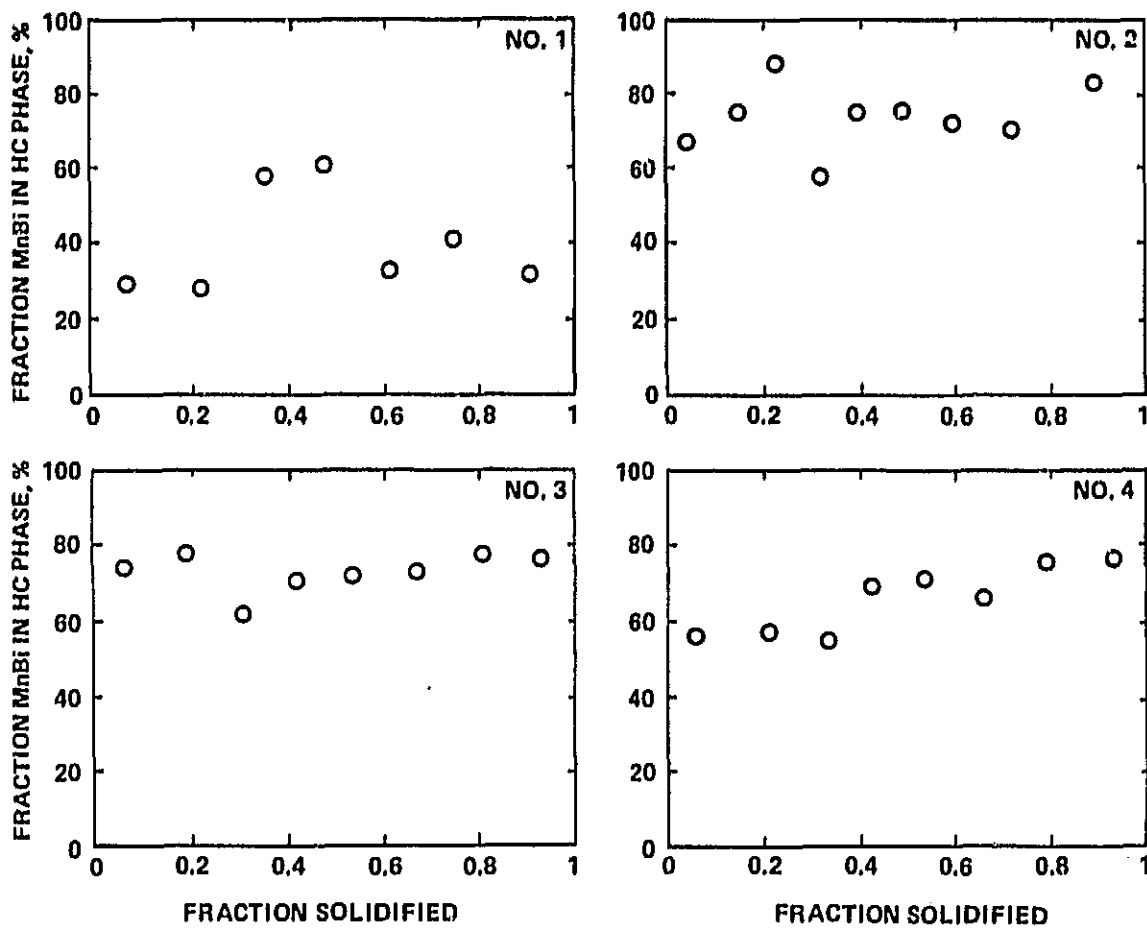
1330-015(T)

Fig. 15 Fraction of MnBi in the HC Phase vs Fraction Solidified for Flight Samples

scatter, after approximately the initial f = 0.37 in low-ḡ, both the
macrosegregation and fraction HC phase curves are similar to those of the
ground-based samples in Fig. 11 and 13. Quantitative analysis of
microstructures in non-low-ḡ cooperatively grown sections of flight samples
No. 3 and 4 are represented in Table 2 and show <d>-values somewhat larger
than the results from ground-based sample No. 4. This may be due to gravity
levels in excess of normal earth gravity at the latter stage of
solidification. Values of <λ> were statistically identical.

Flight sample No. 2 is an interesting Mn-rich sample which solidified
cooperatively over its entire length. Figure 14 shows the macrosegregation of
this sample over its length and presents an unusual situation. X-ray
fluorescence and magnetic measurement determinations of the Mn concentration
do not agree. Unfortunately, complete fluorescence determinations could not
be made due to unresolved measurement problems. Chemical spectrophotometric
absorbance measurements were used as the most reliable test of total bulk Mn
concentration for two samples. In addition, Table 2 includes Mn concentration
values for two sections of flight sample No. 2 determined by microstructural
analysis. Both this last technique and the magnetic measurement technique use
the assumption of the normal-gravity, equilibrium value of 0.11 w/o Mn in the
Bi solid solution in their calculation of the total Mn content and are
therefore insensitive to any solid solution Mn content changes. This is the
possible source of the differences shown in Fig. 14. Whereas the
microstructurally and magnetically derived Mn concentrations are identical,
these results disagree with X-ray fluorescence and chemical results. The
first magnetic data point and chemical data point of Fig. 14 lie in an initial
transient section of this sample, but the next three magnetic data points
result from sections solidified in the proposed low-ḡ period. In this region
of sample No. 2, the chemical and fluorescence results give statistically
equivalent values, the average of which is 0.89 w/o Mn, quite different from
the magnetic and microstructural value of 0.72 w/o Mn. Therefore, while the
given limited evidence is not conclusive, it is suggested that a metastable,
higher Mn content in the Bi solid solution in low-ḡ would be consistent with
these results. More will be said about this later.

35

Table 2 indicates a considerably smaller mean rod diameter, $\langle d \rangle = 0.50 \pm 0.05$ µm, and mean interrod spacing, $\langle \lambda \rangle = 2.3 \pm 0.3$µm, in the proposed low-$\bar{g}$ region than in high-$\bar{g}$, $\langle d \rangle = 0.77 \pm 0.05$ µm and $\langle \lambda \rangle = 3.2 \pm 0.3$ µm. Micrographs comparing the morphology of these two analyzed cross sections are seen in Fig. 16. Similar reductions in both $\langle d \rangle$ and $\langle \lambda \rangle$ seen previously in low-$\bar{g}$ experiments (Ref. 3 and 4) are consistent with the proposal in the present experiment that the first 0.37 fraction solidified of flight sample No. 2 was indeed solidified in the low-$\bar{g}$ portion of the SPAR X flight, as intended.

36
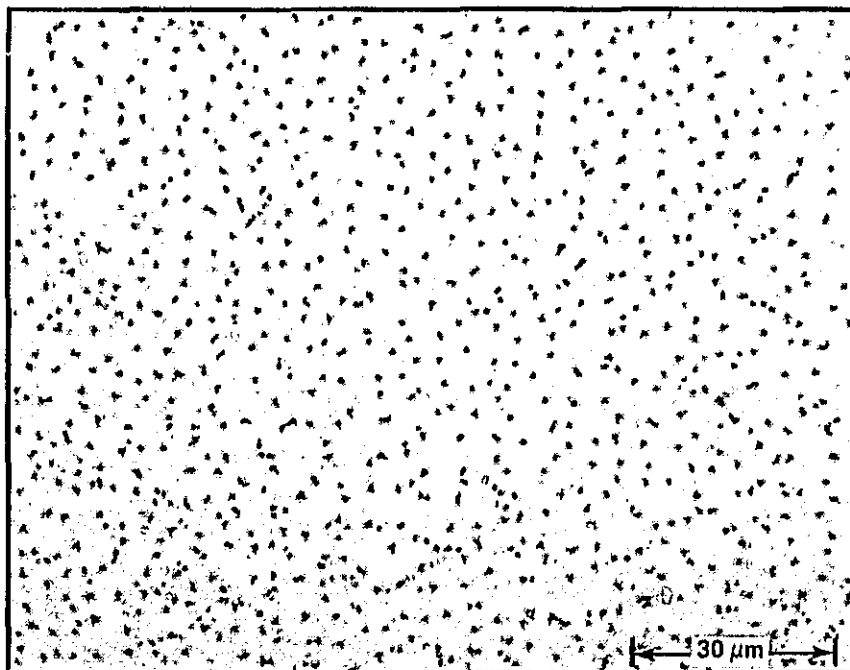
f = 0.20
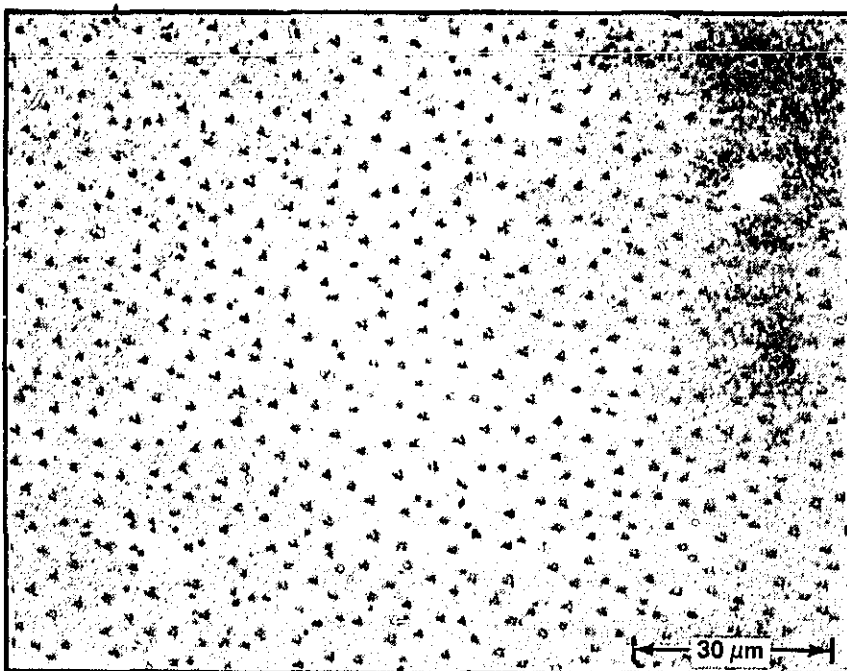
1330-016(T)

f = 0.45

Fig. 16   Comparison of Representative Cooperative Microstructures
of Flight Sample No. 2 from Early & Later Portions of
Sample

37

DISCUSSION

Figure 1 allows the position of the dendritic-to-cooperative transition in samples solidified in the Bi/MnBi off-eutectic system to be predicted for a specific G/V ratio. For the SPAR X experiment, the nominal value of this ratio is $G/V = 0.46 \times 10^5$ °C-s/cm^2. Based on this value, Bi-rich samples should be cooperative for the average solid Mn composition of a section of a sample, C_S, greater than 0.60 w/o Mn, while Mn-rich samples should be cooperative for $C_S < 0.87$ w/o Mn. From Fig. 11, a value of the transition composition, C_{tr}, equal to 0.55 ± 0.02 w/o Mn is reasonably consistent with the results and expectations for both Bi-rich ground-based samples No. 3 and 4. The Mn-rich samples No. 1 and 2 display no discernable macrosegregation in Fig. 11, so that the actual fractional position of the transition in these samples is sensitively dependent on the exact G/V ratio. Sample No. 1 underwent the transition to cooperative growth at $C_{tr} = 0.92 \pm 0.04$ w/o Mn, whereas sample No. 2 was totally dendritic. The ground-based results for this experiment are found to be reasonably consistent with the previous experiments represented in Fig. 1.

In previous work (Ref. 1), Mn macrosegregation was able to be described by the model of Verhoeven and Homer, represented by Eq (3). Here, as discussed in the text following Eq (3), KV is substituted for $p\delta$. If it is noted for ground-based samples No. 3 and 4 that No. 4 shows greater solute redistribution, then a new situation is indicated. With a simplistic argument, the macrosegregation results show, since Mn was rejected at the solidification fronts of these two samples, that the growth down case of sample No. 4, which was unstable thermally but stable solutally, had greater convection in the melt than sample No. 3, which was stable thermally but unstable solutally. This implies that the thermal instability which was present was more important than the induced solutal instability in 1-$\bar{g}$ with these particular solidification processing conditions. This finding is in contrast to the opposite result found in Ref. 1 for lower velocities and gradients and may be due to a decrease in the role of thermal convection relative to solutal convection in 1-$\bar{g}$ as the solidification velocity or thermal gradient increases, or may be an artifact caused by attempting to

38

apply identical convection-solute redistribution arguments to composite and dendritic growth.

In the SPAR IX (Ref. 4) Bi/MnBi eutectic flight experiment, a reduced volume fraction of MnBi was found in the low-gravity processed portion of all samples. That is, sections of the samples grown in low gravity contained 2.95 v/o MnBi, which would correspond to 0.67 w/o Mn, with the normal-gravity processing assumption of 0.11 w/o Mn in the Bi solid solution. Four of these sections have recently been analyzed by chemical spectrophotometric absorbance and found to contain 0.72 ± 0.03 w/o Mn, therefore supporting the suggestion that metastable extensions of the equilibrium normal-gravity phase diagram are operative in low-gravity processing due to interfacial undercooling. With this new result and assuming the densities of the "eutectic" and MnBi remain similar, it can be shown that these sections of SPAR IX samples contained 0.16 w/o Mn in the Bi solid solution, a 41% increase from the 1-$\bar{g}$ equlibrium value. Calculated from the metastable linear extension of the solid solution limit and $\Delta T = 5°C$, a value of 0.18 w/o Mn is obtained. To complete the analysis, however, the metastable, low-gravity processed "eutectic" value cannot be found from SPAR IX results since the solidification of the samples was not completed in low gravity. From the trend of the volume fraction MnBi versus fraction solidified data of the SPAR IX experiment, however, it could be suggested that such a metastable eutectic value would be equal to or greater than the equilibrium value. While the SPAR X results can indicate nothing about a metastable eutectic value since only the first 0.37 fraction of flight sample No. 2 solidified in low gravity, the limited results, specifically, the different composition values found by magnetic and chemical techniques, do support the idea of an increased Mn solubility in the Bi matrix.

At the present time, the concept of a metastable extension of the phase diagram in low gravity seems to account best for MnBi volume fraction changes. Quenisset and Naslain's model, discussed earlier, predicts the necessary increased undercooling in low-gravity processing, as a consequence of reduced convective fluid velocity. Additional undercooling might also be possible from a kinetic term in Eq (2).

SUMMARY & FUTURE EXPERIMENTS

The effects of gravity on Bridgman-Stockbarger directional solidification of off-eutectic Bi/MnBi has been studied in reduced gravity aboard the SPAR X flight experiment and compared to normal-gravity investigations and previous eutectic Bi/MnBi SPAR flight experiments. The results included:

o   Macrosegregation data are consistent with a metastable increase in Mn solubility in the Bi matrix in low-$\bar{g}$, in agreement with previous SPAR findings of MnBi volume reduction.

o   Smaller mean rod diameter and interrod spacing were found in low-gravity compared to earth-gravity solidification.

o   Dendritic-to-cooperative growth transitions in earth gravity agree with a revised supercooling criterion based on previous 1-$\bar{g}$ data.

o   For these processing conditions, thermal instability led to more convection than the induced solutal instability in earth gravity.

o   Heat treatment of samples at $250^{\circ}C$ for 36-48 h resulted in rod shape change from chevron to circular.

Possible mechanisms involving gravity-induced convective fluid flow and metastable phase diagram extensions were proposed to explain the flight experiment findings.

This SPAR X off-eutectic Bi/MnBi solidification experiment was a high risk experiment, based on the very limited low-gravity time period available for processing, and was troubled with additional experimental problems. A longer-term low-gravity, off-eutectic Bi/MnBi solidification experiment is planned for the space shuttle, which will not be subject to severe time limitations and accompanying difficulties. This experiment will be a low

velocity, high gradient experiment with two hypoeutectic and two hypereutectic compositions, which will, for the most part, solidify cooperatively on the ground and on the space shuttle. The objectives of this investigation will be to examine the role of convection in solidification of off-eutectics by determining the effect of low gravity and differing levels of convection on Mn macrosegregation, undercooling, the equilibrium phase diagram, and the detailed accommodation of the Mn content change in rod diameter and interrod spacing.

ACKNOWLEDGEMENTS

REFERENCES

1.   R.G. Pirich, "Gravitationally Induced Convection During Directional Solidification of Off-Eutectic Mn-Bi Alloys," in <u>Matl. Proc. in the Reduced Gravity Envir. of Space</u>, ed. Guy E. Rindone, Elsevier Science Publishing Company, New York, NY, p 593. ,1982).

2.   R.G. Pirich, D.J. Larson, and G. Busch, "Studies of Plane-Front Solidification and Magnetic Properties of Bi/MnBi," <u>AIAA J</u>, Vol 19, p 589, 1981.

3.   R.G. Pirich and D.J. Larson, "SPAR VI Technical Report for Experiment 76-22 – Directional Solidification of Magnetic Composites," Grumman R&D Center Report RE-602, 1980.

4.(a) R.G. Pirich, "SPAR IX Technical Report for Experiment 76-22 – Directional Solidification of Magnetic Composites," Grumman R&D Center Report RE-642, 1982.

4.(b) R.G. Pirich and D.J. Larson, "Influence of Gravity Driven Convection on the Directional Solidification of Bi/MnBi Eutectic Composites," in <u>Matl. Proc. in the Reduced Gravity Envir. of Space</u>, ed. Guy E. Rindone, Elsevier Science Publishing, New York, NY, p 523, 1982

5.   R.G. Pirich, D.J. Larson, and P.N. Adler, "Characterization of the Effects of Plane-Front Solidification and Heat Treatment on the Magnetic Properties of Bi/MnBi Composites," Grumman R&D Center Report RE-663, 1983.

6.   P.S. Ravishankar, W.R. Wilcox, D.J. Larson, "The Microstrucure of MnBi/Bi Eutectic Alloys," <u>Acta Met.</u>, Vol 28, p 1583, 1980.

7.   W.R. Wilcox, K. Doddi, M. Nair and D.J. Larson, "Influences of Freezing Rate Changes on MnBi-Bi Eutectic Microstructure," <u>Adv. Space Res.</u>, Vol 3, p 79, 1983.

8.   V. Baskaran, G.F. Eisa and W.R. Wilcox, "Influence of Convection on Eutectic Microstructure," 2nd Intern. Conf. on Computational Methods and Experimental Methods, Queen Elizabeth II, 1984.

9.   J.D. Verhoeven and R.H. Homer, "The Growth of Off-Eutectic Composites from Stirred Melts," <u>Met. Trans.</u>, Vol 1, p 3437, 1970.

10.   S.H. Gelles, B.C. Giessen, M.E. Glicksman, J.L. Margrave, H. Markovitz, A.S. Nowick, J.D. Verhoeven and A.F. Witt, "Materials Science Experiments in Space," NASA-Lewis Report No. NASA CR-2842, Advanced Copy, p 33, April 1977.

11. S.H. Gelles and A.J. Markworth, "Agglomeration in Immiscible Liquids, Experiment 74-30," in Space Processing Applications Rocket Project, SPAR II-Final Report, NASA Technical Memorandum 78125, p VI-5, November 1977.

12. M.H. Johnston and R.A. Parr, "The Influence of Acceleration Forces on Dendritic Growth and Grain Structure," Met. Trans. B, Vol 13B, p 85, 1982.

13. F.R. Mollard and M.C. Flemings, "Growth of Composites from the Melt - Part I," Trans. Met. Soc. AIME, Vol 239, p 1526, 1967.

14. W.J. Boettinger, F.S. Biancaniello, and S.R. Coriell, "Solutal Convection Induced Macrosegregation and the Dendrite to Composite Transition in Off-Eutectic Alloys," Met. Trans. A, Vol 12A, p 321, 1981.

15. K.A. Jackson, "The Dendrite-Eutectic Transition in Sn-Pb Alloys," Trans. Met. Soc. AIME, Vol 242, p 1275, 1968.

16. M.H. Burden and J.D. Hunt, "The Extent of the Eutectic Range," J. Crys. Growth, Vol 22, p 328, 1974.

17. J.M. Quenisset and R. Naslain, "Effect of Forced Convection on Eutectic Growth," J. Crys. Growth, Vol 54, p 465, 1981.

18. General Electric Company, Space Sciences Laboratory, "Operating Manual for Automated Directional Solidification System," prepared for NASA under contract NAS8-31536, 1978.

19. R.G. Pirich and D.J. Larson, "The Influence of Gravity on Directional Solidification of Eutectic and Off-Eutectic MnBi Alloys," Annual TMS-AIME Mtg. Louisville, KY, 1981.

20. R.G. Pirich, D.J. Larson, and G. Busch, "The Role of Processing Parameters on the Magnetic Properties of Directionally Solidified Bi/MnBi Composites," IEEE Trans. Mag., Vol MAG-15, p 1754, 1979.

21. R.G. Pirich and D.J. Larson, "Magnetic and Metallurgical Properties of Directionally Solidified Bi/MnBi Composites: The Effects of Annealing," J. Appl. Phys., Vol 50, p 2425, 1979.

22. R.G. Pirich, G. Busch, W. Poit, and D.J. Larson, "The Bi-MnBi Eutectic Region of the Bi-Mn Phase Diagram," Met. Trans. A, Vol 11A, p 193, 1980.

23. P.B. Coates and A.C.K. Smith, "Polynomial Representations of Standard Thermocouple Reference Tables," National Physical Laboratory Report QU 36, 1977.

24.   P.B. Coates, "Functional Approximations to the Standard Thermocouple
        Reference Tables," National Physical Laboratory Report QU 46, 1978.

25.   Personal communications with authors of Ref. 4 and 5.